Accepted Manuscript

N-cinnamoylanthranilates as human TRPA1 modulators: Structure-activity relationships and channel binding sites

Arundhasa Chandrabalan, Martin J. McPhillie, Alyn H. Morice, Andrew N. Boa, Laura R. Sadofsky

PII: S0223-5234(19)30206-5

DOI: https://doi.org/10.1016/j.ejmech.2019.02.074

Reference: EJMECH 11166

To appear in: *European Journal of Medicinal Chemistry*

Received Date: 9 January 2019

Revised Date: 27 February 2019

Accepted Date: 27 February 2019

Please cite this article as: A. Chandrabalan, M.J. McPhillie, A.H. Morice, A.N. Boa, L.R. Sadofsky, *N*-cinnamoylanthranilates as human TRPA1 modulators: Structure-activity relationships and channel binding sites, *European Journal of Medicinal Chemistry* (2019), doi: https://doi.org/10.1016/j.ejmech.2019.02.074.

N-Cinnamoylanthranilates as human TRPA1 Modulators: Structure-Activity Relationships and Channel Binding Sites.

Arundhasa Chandrabalan [a,b], Martin J. McPhillie [c], Alyn H. Morice [d], Andrew N. Boa [a,*], Laura R. Sadofsky [b,*]

[a] *Department of Chemistry & Biochemistry, University of Hull, Cottingham Road, Hull HU6 7RX, UK.*

[b] *Centre for Atherothrombosis and Metabolic Disease, Hull York Medical School, University of Hull, Cottingham Road, Hull HU6 7RX, UK.*

[c] *School of Chemistry, University of Leeds, Leeds LS2 9JT, UK*

[d] *Respiratory Medicine, Hull York Medical School, Castle Hill Hospital, Cottingham HU16 5JQ, UK.*

* **Corresponding authors**

Email addresses: a.n.boa@hull.ac.uk (ANB), laura.sadofsky@hyms.ac.uk (LRS)

Graphical Abstract

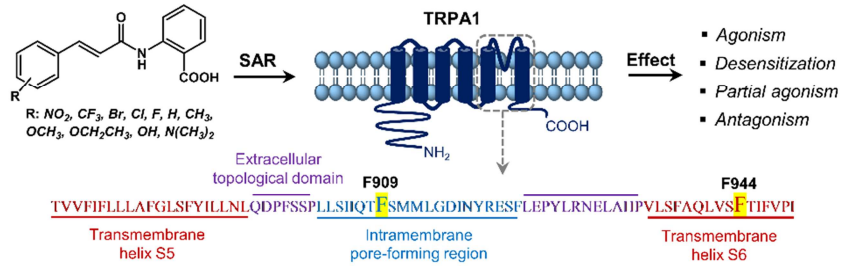

Highlights

N-Cinnamoyl anthranilate derivatives (CADs) are TRPA1 modulators

CADs with electron-withdrawing groups are TRPA1 agonists with desensitizing effects

CADs with strongly electron-donating groups are TRPA1 antagonists

CADs modulate TRPA1 through non-covalent interactions

F944A mutants show reduced sensitivity towards CADs and many other TRPA1 modulators

Abstract

The transient receptor potential ankyrin 1 (TRPA1) channel is a non-selective cation channel, which detects noxious stimuli leading to pain, itch and cough. However, the mechanism(s) of channel modulation by many of the known, non-reactive modulators has not been fully elucidated. *N*-cinnamoylanthranilic acid derivatives (CADs) contain structural elements from the TRPA1 modulators cinnamaldehyde and flufenamic acid, so it was hypothesized that specific modulators could be found amongst them and more could be learnt about modulation of TRPA1 with these compounds. A series of CADs was therefore screened for agonism and antagonism in HEK293 cells stably transfected with WT-human (h)TRPA1, or C621A, F909A or F944A mutant hTRPA1. Derivatives with electron-withdrawing and/or electron-donating substituents were found to possess different activities. CADs with inductive electron-withdrawing groups were agonists with desensitizing effects, and CADs with electron-donating groups were either partial agonists or antagonists. Site-directed mutagenesis revealed the CADs do not undergo conjugate addition reaction with TRPA1 and reveal that F944 is a key residue involved in the non-covalent modulation of TRPA1 by CADs, as well as many other structurally distinct non-reactive TRPA1 ligands already reported.

Keywords: transient receptor potential ankyrin 1; TRPA1; TRP; *N*-cinnamoylanthranilic acid; tranilast; calcium signaling; binding site; non-covalent

Abbreviations Used

$[Ca^{2+}]_i$, intracellular calcium ion; CAD, *N*-cinnamoylanthranilic acid derivative; hTRPA1, human transient receptor potential ankyrin 1; hTRPM8, human transient receptor potential melastatin 8.

54

1. Introduction

The human transient receptor potential ankyrin 1 (hTRPA1) channel [1] is predominantly expressed in the primary afferent (sensory) neurons [2] including trigeminal [3], dorsal root [4] and nodose ganglia, [5] and acts as a detector of chemical, mechanical and thermal stimuli [6]. TRPA1 is known to be involved in pain, itch, [7, 8] inflammatory diseases like arthritis [9], chronic obstructive pulmonary disease (COPD), and other respiratory diseases including chronic cough and asthma [6, 10]. There are many compounds known to modulate TRPA1, among them compounds containing reactive electrophilic groups that activate the channel through covalent modification of cysteine or lysine residues at the *N*-terminus of the protein [11, 12]. However, TRPA1 is also modulated by compounds through non-covalent interactions only. Mutagenesis and chimeric approaches have been utilized to elucidate the interactions of individual non-reactive chemicals with the channel [12-17]. However, the non-covalent mechanism(s) of modulation (activation or blocking) by compounds with distinct structures are currently much less well determined, hindering our understanding of the role of TRPA1 in diseases, and development of drugs targeting the channel.

Analogues of *N*-cinnamoylanthranilic acid (**1**) have shown a range of biological activities, including anti-allergic, anti-histaminic, anti-inflammatory, anti-asthmatic, [18, 19] anti-oxidant, [20] anti-fibrotic [21], anti-proliferative, [22] anti-cancer, [23] anti-platelet, [24] anti-coagulant [25] and as modulators of B-cells and T-cells, [26, 27], and are under investigations for several medicinal applications. The derivative *N*-(3,4-dimethoxycinnamoyl)anthranilic acid (**11**, Tranilast™ or Rizaben™) is an anti-inflammatory drug that has been used in South Korea and Japan for over twenty years to treat allergic diseases such as bronchial asthma, allergic rhinitis, hypertrophic scars and scleroderma [18, 21, 28]. *N*-cinnamoylanthranilate derivatives (CADs) also contain structural elements from two classes of known TRPA1 modulators, namely the α,β-unsaturated carbonyl moiety found

in the agonist cinnamaldehyde (CA), [29] and the anthranilate moiety found in the agonist flufenamic acid (FFA) and related fenamates [30]. It was therefore anticipated that discovery of CAD agonists or antagonists of TRPA1 could be used to learn about the modulation of the channel by non-reactive compounds.

CADs have previously been shown to inhibit other TRP channels. For example *N*-(*p*-amylcinnamoyl)anthranilic acid (ACA), a PLA_2 inhibitor, [31] was characterized as a novel TRPM2, TRPM8, TRPC3, TRPC6 and TRPV1 channel blocker [32]. Similarly, *N*-(3-methoxyphenyl)-4-chlorocinnamide (SB366791) selectively blocks TRPV1 [33], yet is inactive against TRPM8 [34]. The anthranilates 5-nitro-2-(phenethylamino)benzoic acid (NPEB), 5-nitro-2-(phenethylamino)benzamide (NPBA) and 5-nitro-2-(3-phenylpropylamino)benzoic acid (NPPB), the latter which bears some overall similarity to CAD **1**), selectively activates TRPA1 [35]. Therefore, to investigate both the structure-activity relationship (SAR) and pharmacology of CADs as TRPA1 modulators, we set out to synthesize and screen a series of compounds against TRPA1-transfected HEK293 cells.

2. Materials and Methods

2.1 Materials.

2.1.1 Commercial TRPA1 modulators. Cinnamaldehyde (CA, ≥ 95 %, natural), acrolein (ACR, analytical standard), allyl isothiocyanate (AITC, analytical standard), menthol (99 %), (-)-menthol and 5-nitro-2-(3-phenylpropylamino)benzoic (NPPB) were purchased from Sigma-Aldrich. Calcimycin (calcium ionophore, A23187), thymol (> 99.5 %), carvacrol (98 %), eugenol (99 %), cyclohexylcarbamic acid 3′-carbamoyl-biphenyl-3-yl ester (URB597, ≥ 98 %), (-)-nicotine (≥ 99 %), *N*-(*p*-amylcinnamoyl)anthranilic acid (ACA, ≥ 98 %), probenecid, 4-(4-chlorophenyl)-3-methylbut-3-en-2-oxime (AP18) and 2-(1,3-dimethyl-2,6-dioxo-1,2,3,6-tetrahydro-7*H*-purin-7-yl)-*N*-(4-isopropylphenyl)acetamide (HC030031) were

purchased from Sigma-Aldrich. (1*E*,3*E*)-1-(4-fluorophenyl)-2-methylpent-1-en-3-one oxime (A967079), *N*-(3-aminopropyl)-2-((3-methylbenzyl)oxy)-*N*-(thiophen-2-ylmethyl)benzamide hydrochloride (AMTB.HCl) and SB366791 were purchased from Tocris Bioscience. Ethyl ((1*R*,2*S*,5*R*)-2-isopropyl-5-methylcyclohexane-1-carbonyl)glycinate (WS5) was from Millennium Specialty Chemicals Inc., Procter & Gamble, flufenamic acid (analytical standard) was from Fluka Analytical, mefenamic acid (98 %) was from Johnson Matthey Company and diclofenac (> 98 %) was from Tokyo Chemical Industry. Nordihydroguaiaretic acid (NDGA) and farnesylthiosalicylic acid (FTS) were purchased from Santa Cruz Biotechnology. The structures of these various TRPA1 modulators are shown in Figure 1. The stock solutions of the compounds were made and serially diluted to lower half-log scale concentrations in dimethyl sulfoxide (DMSO, 100 %, analytical reagent grade, Fisher Scientific), and thus the concentration of DMSO was maintained constant in a given total volume of sample.

2.1.2 Chemistry.

The Orion Corporation-disclosed aryl sulfonamide derivative (*S*)-*N*-(4-chlorobenzyl)-1-((4-fluorophenyl)sulfonyl)pyrrolidine-2-carboxamide (ASD) [36], the series of CADs and related derivatives were synthesized in-house using standard methods (see Supporting Information for details). Briefly, three synthetic routes were followed to synthesize the CADs. In one approach, the cinnamic acid derivative was converted to its corresponding acid chloride, which was coupled to methyl anthranilate, and the resulting methyl *N*-cinnamoylanthranilate was then hydrolyzed to yield the corresponding *N*-cinnamoylanthranilic acid derivative (Scheme 1). In the second approach, Meldrum's acid was reacted with anthranilic acid to produce 2-[(carboxyacetyl)amino]benzoic acid, which was then condensed with a benzaldehyde derivative *via* a piperidine-catalysed Knoevenagel condensation, producing *N*-

cinnamoylanthranilate as the piperidinium salt which was acidified to yield the final product (Scheme 2). In the third approach, a secondary amino acid was reacted with cinnamoyl chloride under basic conditions, and the resulting salt was acidified to yield the product (Scheme 3). Compound purity was assessed by satisfactory CHN combustion elemental microanalysis, ^{1}H and ^{13}C NMR spectroscopy, and a constant melting point. Chemical and spectroscopic data obtained for compounds synthesized (see Supporting Information) agreed closely with that reported, where available, in the literature. Stock solutions of these compounds were prepared as described above (Section 2.1.1).

2.2 Cell culture. HEK293 cells stably transfected with either pcDNA3.1(+) constructs containing cDNA for hTRPA1 [37], hTRPM8 [38], hTRPA1 mutants or pcDNA3 (mock) were grown in Dulbecco's Modified Eagle's Medium (DMEM) containing 25 mM 4-(2-hydroxyethyl)-1-piperazine ethanesulfonic acid (HEPES) and 4.5 g l^{-1} glucose, supplemented with 2 mM L-glutamine, 100 U ml^{-1} penicillin, 100 U ml^{-1} streptomycin (all from Lonza), 10 % v/v heat inactivated Fetal Bovine Serum (Life Technologies) and 0.25 mg ml^{-1} geneticin (G418 Sulfate, Corning). The cells were grown in T75 tissue culture flask (Greiner Bio-One CELLSTAR) in a humidified cell culture incubator with 5 % CO_2 at 37 °C. When the cells reached ~90 % confluence, they were harvested in phosphate buffered saline (PBS, Sigma-Aldrich) solution and centrifuged at 205 × *g* for 4 min for calcium signaling experiments.

2.3 Calcium signaling. The modulatory effects of the CADs were evaluated on hTRPA1, hTRPM8 and pcDNA3 (mock) transfected-HEK293 cells using a fluorescence-based calcium signaling assays at room temperature, either in the cuvette-based system or a micro-well plate system as described below.

Cuvette-based system: A previously reported protocol was followed [38]. Briefly, the cell pellet obtained from ~90 % confluence in T75 flask was resuspended in 0.5 ml complete DMEM and incubated with 2.5 µl of 2.5 µg µl^{1} Fluo-3AM fluorescent dye ($\lambda_{Ex/Em}$ 506/526 nm, Life Technologies) for 30 min at room temperature with gentle rotary mixing (50 rpm). The cells were washed with PBS by centrifuging as before, and the pellet was resuspended in isotonic assay buffer [38] (10 mM HEPES, 145 mM NaCl, 5 mM KCl, 1 mM $MgCl_2.6H_2O$, 1 mM $CaCl_2$ and 10 mM D-(+)-glucose made in double distilled water, and pH was adjusted with NaOH) at a density of 5×10^6 cells ml^{-1}. The cell suspension (100 µl) was added to cuvettes containing the assay buffer (1.9 ml). The assays were carried out using a PTI fluorometer with FelixGX version 4.2.2 software. The amount of $[Ca^{2+}]_i$ released upon activation of TRP channels were measured as a real-time-based fluorescence spectrum. The baseline of a spectrum was recorded for 20 s before the addition of a test compound (agonist) and the response was recorded for another 90 s, followed by the addition of calcimycin (2 µM) and recording for further 30 s. In antagonist assays, the standard antagonist, the vehicle control or the test compounds were pre-incubated with cells for 10 min prior to the addition of a standard agonist, and the spectrum was recorded as before.

Micro-well plate system: 96-Well cell culture microplates (black polystyrene, flat µClear bottom, Greiner Bio-One) were coated with poly-D-lysine (PDL, MW 70-150 kDa, Sigma-Aldrich, 50 µg ml^{-1} prepared in sterile PBS) as follows: PDL was added to the wells (200 µl cm^{-2}) and incubated for an hour at room temperature, excess PDL solution was aspirated and the wells were washed with PBS (2 × 100 µl per well), and air-dried at room temperature for 2 h in a safety cabinet. Cell suspension (200 µl of 12500 cells per well in complete DMEM) was added to the wells and incubated in the cell culture incubator (95% air and 5% CO_2 at 37 °C) for 48 h to yield a final concentration of 5×10^4 cells per well. The culture medium was

replaced with 100 µl of 2 µM Fluo-4AM [$\lambda_{Ex/Em}$ 494/506 nm (Life Technologies), diluted in phenol red-free DMEM (Life Technologies) from DMSO stock] and incubated in the dark at room temperature for 45 min. The cells were rinsed with PBS (2 × 100 µl per well), and the isotonic assay buffer (100 µl per well for agonist assays or 50 µl per well for antagonist assays) was added to the wells. In antagonist assays, the cells in 50 µl buffer were incubated with 50 µl antagonists for 10 min before assaying. The assays were carried out using a FlexStation3 Molecular Devices with the SoftMax Pro Software version 5. The protocol utilized was adapted from the literature [39, 40]. Briefly, the real-time-based fluorescence spectra were recorded using the read-mode/type: Flex fluorescence (RFUs) bottom-read. An excitation and emission wavelengths of 485 and 538 nm were used for measurements with 530 nm auto cut-off. Each spectrum was recorded for a total run time of 240 s, where the baseline was recorded for 20 s, and at the end of which the first addition (compound) was made followed by the second addition (calcimycin) at 180 s.

To determine the reversibility of an antagonist, after pre-incubation, the cells were washed with the assay buffer and resuspended in fresh assay buffer, and the response for the TRPA1 standard agonist CA (30 µM) was examined. Competitiveness of an antagonist was determined by pre-incubating cells with the test antagonist compound of a known concentration for 10 min and by considering the shift in the dose-response curve of CA with and without the inhibitor.

2.4 Graphical and statistical analyses. The agonism and antagonism responses were calculated either as a percentage of calcimycin or a standard agonist respectively, using the differences in the maximum and minimum relative fluorescence unit (ΔRFU) values. Initial screening results correspond to three independent experiments (N = 3), and the errors

reported are the standard error of the mean (SEM). The dose-response curves were plotted and analyzed using GraphPad Prism version 5.03, and the values of $logEC_{50}$ and $logIC_{50}$ were obtained with their SEM. Each data point on a dose-response curve corresponds to the mean of three independent experiments (N = 3), performed either in duplicates (n = 6) or triplicates (n = 9), with their SEM. The responses were normalized by subtracting the noise/response obtained for the vehicle control (DMSO). In antagonist assays, the maximum response was obtained by normalising the standard agonist response to 100 %. Thus, in antagonist assays, a higher percentage value indicates a lower inhibitory effect by the test compound. To determine statistical significance between groups, the one-way analysis of variance (ANOVA) at $p < 0.05$ was carried out.

The standard agonists and antagonists for positive controls were chosen, based on the ion channel specificity and potency of the ligands, and a concentration near or above EC_{50} or IC_{50} were used in the assays. The standard agonists used for the hTRPA1 channels were CA (30 µM), ACR (30 µM) or AITC (10 µM), and for hTRPM8 was WS5 (1 µM). The standard antagonists used were the potent TRPA1 selective A967079 (100 or 300 nM) and TRPM8 selective AMTB.HCl (1 or 3 µM).

2.5 Indirect measure of inertness towards covalent modification. As CADs could conceivably react with the TRPA1 *via* a conjugate addition processes, we wanted first to disprove that they reacted with a model nucleophile in the absence of the channel (see similar studies in [41]). Thus compound **1a** (4 equiv., 226 mM) and *N*-acetyl-L-cysteine methyl ester (1 equiv., 56 mM) or *N*-acetyl-L-cysteine (1 equiv., 61 mM) in d_6-DMSO were mixed together, and the progress of any reaction was monitored using ^{1}H NMR spectra recorded at 25 °C and at known time intervals.

2.6 Site-directed mutagenesis. hTRPA1 mutants C621A (site of covalent modification) [13], F909A or F944A (sites of non-covalent interaction identified by [16, 17]) cDNAs were produced using a QuikChange Lightening Site-Directed Mutagenesis kit (Agilent Technologies) as instructed in their manual, using pcDNA3.1(+) as the template and hTRPA1 primers containing the mutants (synthetic oligonucleotides purchased from Eurofins Genomics MWG Operon). Briefly, hTRPA1 mutants strands were synthesized by performing 18 cycles of PCR, followed by digestion of the parental- and hemi-methylated supercoiled dsDNA in the amplified products with *Dpn* I restriction enzyme. The amplified DNA was then transformed into XL10-Gold ultracompetent cells (*E. coli*) treated with β-mercaptoethanol. Plasmid DNA was isolated from the *E. coli* and purified using a NucleoSpin® Plasmid DNA purification miniprep kit (Macherey-Nagel) according to the manufacturer's protocol. The dsDNA samples were quantified (NanoDrop Lite Spectrophotometer, Thermo Scientific), and sequenced (Eurofins Genomics DNA sequencing service) and compared against the parent hTRPA1 sequence (sequence ID: Y10601) to confirm the mutations.

HEK293 cells were transfected with the hTRPA1 mutants dsDNA (0.3 µg µl^{-1}) separately using FuGENE® 6 Transfection Reagent (Promega) as per the manufacturer's instructions. The transfection reagent FuGENE and DNA were added in 3:1 ratio. G418 (0.5 mg ml^{-1}) resistance cells were then expanded in T25 and T75 flasks sequentially. The transfected cells were single cell cloned by serial dilution in a 96-well cell culture plate following Corning's procedure. Monoclonal cells were transferred to a 6-well cell culture plate and then into T75 flasks for expansion. The cells were characterized with known hTRPA1 specific agonists and antagonists using the calcium signaling technique and compared against the WT-hTRPA1

255 responses to determine the level of TRPA1 protein stably expressed in the transfected
256 HEK293 cells. The known TRPA1 ligands characterized in the hTRPA1 mutants were CA,
257 AITC, ACR, menthol, thymol, carvacrol, eugenol, FFA, MFA, DCF, NPPB, URB597, FTS,
258 (-)-nicotine, NDGA, probenecid, HC030031, AP18, A967079 and ASD.
259
260 **2.7 Electrophysiology.** Experiments involving animals were performed by IR Pharma
261 (London, UK). Experiments were performed in accordance with the U.K. Home Office
262 Guidelines for Animal Welfare based on the Animals (Scientific Procedures) Act of 1986 and
263 the ARRIVE guidelines [42]. Vagus nerves of eight male Dunkin-Hartley guinea pigs
264 (300-400 g) were isolated, characterized and experimented as described previously [43, 44].
265 Compound stock solutions were prepared in DMSO and diluted 1000× in Krebs-Henseleit
266 (KH) buffer. The depolarization was recorded in mV. To determine if a compound caused
267 activation of the nerve, non-cumulative concentration responses to potential tussive stimuli
268 were carried out. A control response to the TRPV1 agonist capsaicin (1 µM) was carried out
269 to determine nerve viability, following which the nerve was stimulated with single
270 concentrations of a test compound for 2 min. After application of each concentration of the
271 compound, the nerve was washed with KH buffer until it returned to baseline, and this was
272 repeated with the full range of concentrations. A similar stimulation was also carried out with
273 the vehicle control (DMSO). A further control response to TRPA1 agonist acrolein (300 µM)
274 was carried out at the end of the experiment to determine nerve viability.
275
276 In order to study antagonism, the nerve was exposed to the agonist ACR (300 µM) for 2 min
277 and washed with KH buffer until the response returned to baseline. This was repeated to
278 provide two control agonist responses. The nerve was then pre-treated with a test compound
279 for 10 min, and then re-stimulated with ACR (300 µM) for 2 min 20 s (the additional 20 s

was to allow for the changeover of stimuli) to assess if the compound was able to affect the magnitude of the depolarization induced by the ACR. Following a brief washout, the nerve was exposed to ACR (300 µM) for 2 min to provide a recovery response to ensure nerve viability and that the compound was washed off.

3. Results

3.1 Calcium signaling. The CADs were evaluated in HEK293 cells stably transfected with hTRPA1, hTRPM8 or pcDNA3 using a fluorescence-based calcium signaling technique. Agonism of the compounds were measured by assessing the Ca^{2+} influx in TRPA1-HEK293 cells upon exposure to the test compounds relative to calcimycin (calcium ionophore, A23187), and antagonism of the compounds were measured by the ability of the test compounds to antagonize the agonism of a standard agonist. Hence, the agonism and antagonism responses of the compounds are presented as the percentage of calcimycin and standard agonist, respectively (Tables 1 and 2). The vehicle control (0.2 or 0.4 % DMSO) had no significant activity in hTRPA1 and in mock transfected-HEK293 cells (data not shown), but had a slight antagonising effect (inhibits ~20 % of WS5 response) in hTRPM8.

Carboxylic acid-containing compounds were evaluated as their corresponding carboxylate salt due to the isotonic assay buffer (pH 7.4). Even so, for some derivatives insolubility in the buffer at higher concentrations (300 µM, or in some cases >100 µM) prevented completion of the dose-response curve (Fig. 3). Most of the CAD esters were partially soluble or insoluble above 3 µM, and hence screening at higher concentrations was not possible. The CADs, **14** and **15** autofluoresced in the wavelength region of Fluo-3 and Fluo-4 dyes, so screening was not possible. Due to broad absorption ranges for these two CADs other long-wavelength calcium dyes were found not to be suitable either.

3.2 CAD Structure-Activity Relationship in hTRPA1. In the initial screening of *N*-cinnamoylanthranilic acids (Table 1), the CADs **1-10**, **20** and **21** showed ≥25 % agonism at 30 μM and ≥50 % inhibition at 100 μM. The agonists **2**, **3**, **20** and **21** showed weak antagonism in the initial screen, relative to other antagonists (e.g. **4**, **5** and **6**), so full inhibition curves were not done and IC_{50} values were not calculated. The CADs **11**, **12**, and **16-19** showed weak agonism (<25 %) whereas CAD **13** showed no agonism. However, the CADs **11-13** showed ≥40 % inhibition, and **16-19** showed weak inhibitory effect (<30 %). In the initial screening of methyl *N*-cinnamoylanthranilates (Table 2), all the evaluated esters, including **1a**, **3a-8a**, **13a-15a**, and **20a-22a**, were agonists (Table 2). Most of the methyl *N*-cinnamoylanthranilate esters at 3 μM showed a similar level of agonism to that of their corresponding *N*-cinnamoylanthranilic acid derivatives at 30 μM. However, apart from **20a** and **21a**, none of the esters showed antagonism. Dose-response curves were carried out for *N*-cinnamoylanthranilic acids that showed higher than 25 % agonism at 30 μM, and for those which had high antagonism and partial agonism. As can be seen from the curves, the effects observed were dose-dependent (Fig. 3).

The halogenated CADs **4** and **5**, with a bromo or chloro substituent at the *para*-position, had similar potency, whereas the fluorinated CAD **7** showed an increase in EC_{50} and IC_{50}, relative to other halogens in the series. As the halogenated CADs **4-7** showed potent agonism and antagonism, it was thought that they might possess desensitising effects following activation of the channel. This was confirmed by recording the real-time spectra for 10 min (Fig. 4a,b). Since CA and FFA are known to have desensitising effects, [30, 45] they were also evaluated along with the CADs for comparison. At the concentration eliciting a maximum response, the elevated Ca^{2+} level caused by the agonism was sustained (Fig. 4b),

and at a submaximal concentration the effect dropped over 200-300 s. On continuous exposure to an agonist a diminished response was obtained (Fig. 4c-f), due to desensitization of the channel (see [30]). For the CADs tested at 10 µM the agonism response dropped back nearer to the spectral baseline within 10 min of administration and desensitized the agonism of the CA (30 µM) standard agonist (Fig. 4c-f). Due to this bimodal activity, potent agonism and desensitising effect, a washout experiment was carried out to examine the reversibility of the compounds. The desensitising effect shown by the halogenated CADs on hTRPA1 was found to be reversible up to 10 µM for **4** and **5**, and up to 30 µM for **6** and **7**, and were irreversible at higher concentrations (Fig. 5).

The CADs with a methyl (**8**) or methoxy (**10**) group possessed similar agonist activity at 30 µM in the initial screening. However, on comparing the EC_{50} of **8** and **10**, CAD **8** appeared to be less potent. Disubstituted CADs **11** and **12** with electron donating groups (EDGs) exhibited partial agonist and antagonist activities, whilst **13** showed only an antagonistic effect and no agonism below 100 µM. Nevertheless, the disubstituted CADs **11** and **12** were less potent antagonists compared to the monosubstituted **13**.

Ortho-substituted CADs **6** and **9** were less efficacious, relative to their corresponding *para*-substituted analogues **5** and **10**. In addition, α,β-saturated derivatives **16** and **17** showed poor activity at 30 µM compared to the corresponding CADs **1** and **10** with an α,β-unsaturation. The compounds **18** and **19** with a non-planar ring replacing the anthranilate moiety showed weak responses relative to the parent compound **1**. The α-substituted CADs either with a methyl or phenyl group were more potent agonists (**20** and **21**) relative to the unsubstituted CAD (**1**). Among the α-substituted CADs **20** and **21**, and unsubstituted CAD **1**, the derivative **21** showed pronounced agonist potency.

The *N*-cinnamoylanthranilic acid methyl esters evaluated in hTRPA1 at 3 µM (Table 2) showed a similar level of agonism to their corresponding *N*-cinnamoylanthranilate derivatives at 30 µM (Table 1), but there were no considerable antagonism shown by the esters, except for **20a** and **21a** with desensitising effects.

3.3 Channel selectivity. To determine the channel selectivity of CADs, they were assessed in pcDNA3 mock-HEK293 cells for agonism, and in hTRPM8-HEK293 cells for both agonism and antagonism. The CADs, evaluated at 30 and 100 µM, and CAD methyl esters, at 3 µM, did not show any response in the negative control pcDNA3 mock-transfected HEK293 cells (N = 3, data not shown).

There was no agonism seen for any CADs in hTRPM8-transfected HEK293 at the concentrations 30 and 100 µM of *N*-cinnamoylanthranilates, and 3 µM of methyl *N*-cinnamoylanthranilates (data not shown), except for **21** and **21a** which exhibited weak agonism (Tables 1 and 2). The majority of the compounds which were hTRPA1 agonists, were weak hTRPM8 antagonists at high concentrations. Dose-response curves were carried out for, **3**, **4**, **6**, **9**, **20** and **22a**, that showed high antagonism (Tables 1 and 2), amongst which **22a** was the most potent hTRPM8 antagonist with IC_{50} 10 µM (Fig. 3g). In addition, it was observed from the IC_{50} values that the CAD **4**, which showed antagonism in both hTRPA1 and hTRPM8, was more potent in hTRPA1. However, the CADs **6** and **9** had only a 10 µM difference in the IC_{50} values obtained against hTRPM8 and hTRPA1 (Table 1).

3.4 Determination of possible binding sites through mutagenesis studies.

Binding site. CADs could undergo covalent modification due to the presence of an α,β-unsaturated carbonyl group. Previously we have used NMR scale model reactions of reactive molecules with cysteine as a quick way of gauging susceptibility of a molecule towards covalent modification of a TRPA1 cysteine residue, and good correlation with agonism levels has been observed [41]. Therefore, the propensity of CADs to react through conjugate addition of the thiol group in cysteine (*N*-acetyl-L-cysteine methyl ester or *N*-acetyl-L-cysteine) to the α,β-unsaturated double bond was evaluated for the representative CAD **1a** (Scheme S4, Supporting information) using a proton NMR time study. This CAD showed no reactivity to the thiol group of cysteine in d_6-DMSO, as monitored by changes in intensity or appearance of new peaks in the NMR spectrum over 6 h (data not shown). However, to rule out covalent modification of the channel completely, studies of CADs with C621A mutants were conducted as part of a study to determine the binding site of the CADs.

CADs and a range of other known hTRPA1 active ligands were characterized in HEK293 cells stably transfected with hTRPA1 mutants C621A, F909A or F944A at concentrations corresponding to the maximum response or closer to the EC_{50} or IC_{50} obtained in wild-type (WT)-hTRPA1 HEK293 cells. The EC_{50} and IC_{50} values obtained in the WT-hTRPA1 (Table 3) were broadly consistent with the values found in the original reports, given possible variations in the assay methods, conditions, species and/or cell lines. Significantly reduced agonism was obtained, as expected, for the electrophilic compounds, CA, AITC and ACR in the mutant C621A-hTRPA1. Reduced agonism was also observed for the non-reactive compounds menthol, carvacrol, FFA, DCF, NPPB, FTS, probenecid and **22a**, relative to the responses obtained in WT-hTRPA1-HEK293 (Fig. 6a-e). With the exception of the saturated analogue **22a**, CADs produced increased responses relative to that observed in the WT-hTRPA1 (Fig. 6e).

A967079, AP18, CAD **13** and ASD all had reduced antagonistic responses in F909A-hTRPA1 expressing HEK293 cells relative to WT-TRPA1 expressing cells (Fig. 6f). No reduction in antagonism was observed for HC030031 in the F909 mutant. Menthol and carvacrol also showed a reduced agonist effect in the absence of F909, however most of the other compounds showed a significantly increased agonist response in this mutant compared to the WT (Fig. 6a-e).

In the mutant F944A-hTRPA1 HEK293 cells a significant drop in activity was found for ACR, menthol, carvacrol, eugenol and FFA, NDGA, probenecid, CADs **3** and **22a**, **8** and **20**, ACA, A967079 and AP18 and ASD, relative to the responses in WT-hTRPA1 (Fig. 6). In the case of ACA and **3**, reduced responses were obtained only at a lower concentration (10 µM) and not at a higher concentration (30 µM), as shown in Fig. 6e.

3.5 Electrophysiology. The agonist and antagonist effects of the compounds, **3** and **5** at 100 µM, and **13** at 300 µM, were tested on fully characterized isolated guinea pig vagus nerve preparations. The compounds showed a small degree of activation of the vagus nerve (Fig. 7a-c), with **3** having the largest effect as in the hTRPA1-HEK293 cells. However, the potency of the responses obtained in tissue (nerve) did not compare to those obtained in HEK293 cells overexpressing hTRPA1.

4. Discussion

TRPA1 is activated by a wide range of stimuli. Some of the chemical modulators activate the channel *via* covalent modification of specific residues on the *N*-terminal of the channel [6, 11, 12], however a large number do not possess the reactive groups to do likewise [12]. Here we have studied CADs as modulators of TRPA1 activity, and investigated where these compounds bind to the channel. Comparing trends in the SAR of the acid CADs against

hTRPA1, we noted the parent (unsubstituted) compound **1** had a moderate agonistic effect, and the electron withdrawing group (EWG)-substituted CADs **2** and **3** were more potent agonists. The halogenated CADs (**4** - **7**), with inductive electron withdrawing but lone pair donating properties showed potent agonism with desensitising effect, and the CADs **8** - **10**, with a weak/moderate electron donating group (EDG), showed bimodal activity, that is they possessed partial agonism and antagonism. As the electron donating nature of the EDG becomes stronger the agonism of the compounds decreased and became antagonists (**11** - **13**). The potent agonism and antagonism of the halogenated CADs was due to a desensitising effect following activation of the channel, as was also shown for FFA [30]. This was reversible at low CAD concentration (<10μM) but irreversible at higher concentrations.

α,β-Saturated analogue **16** and **17** showed poor activity compared to the corresponding α,β-unsaturated CADs. However it is interesting to note that the related, flexible derivative NPPB, a classic chloride ion channel antagonist, is a sub-micromolar agonist of TRPA1 [35]. Unlike the CADs studied, NPPB possesses a nitro group in the anthranilate ring, and replacing the anthranilate moiety in our CADs with a saturated cyclic amino acid (**18** and **19**) produced weak responses. This suggests that the anthranilate moiety probably plays a key role in the activity of the CADs.

The agonism of structurally related compounds in the literature including ACA, an inhibitor of several TRP channels, [32], and SB366791, a selective TRPV1 antagonist [33, 34], were evaluated against hTRPA1-HEK293. ACA [32], with a 4-pentyl substituent, activated hTRPA1 potently relative to the 4-methyl substituted CAD **8**. Despite being similar to CAD **5** (but lacking COOH on the *N*-aryl ring), SB366791 had no agonism in hTRPA1 (data not shown). A similar trend to that observed for the EWG and EDG substituted CADs, has also been reported for modulation of hTRPA1 by substituted benzylidenemalononitriles. [46]

HEK293 cells endogenously express a number of ion channels and receptors, including purinoceptors ($P2Y_1$ and $P2Y_2$) [47], voltage-gated potassium channels [48, 49], sodium channels (β1A and $Na_v1.7$) [50, 51], sphingosine-1-phosphate receptors (Edg-1, Edg-3 and Edg-5) [52], calcium channels [53] including TRPC1, TRPC3, TRPC4, TRPC6 and TRPC7 [54, 55], and M_3 muscarinic acetylcholine receptor [56]. The CADs and methyl *N*-cinnamoylanthranilate, did not activate the negative control mock-transfected HEK293 cells, proving that in TRPA1-HEK293 cells the compounds were selective to TRPA1.

TRPM8, a cold-sensitive channel [57], is stimulated by a number of TRPA1 modulators [58, 59]. Therefore, CADs were evaluated against stably transfected hTRPM8-HEK293 cells for selectivity between these two channels. CADs active in hTRPM8 contained either a halogen, an *ortho*- or an α-substituent. Interestingly, most of the TRPA1 agonists were hTRPM8 antagonists at higher concentrations. However assays against a range of other ion channels are necessary to confirm overall channel selectivity.

Looking at the physicochemical properties (Table S1) among similar analogues, compounds possessing a higher clogP were the more potent agonists, as also seen in examples in the literature [35, 60]. Generally, the CADs with a higher number of hydrogen bond donors and acceptors, larger topological polar surface area and logS, and lower logP had greater inhibitory effects with poor or no hTRPA1 agonism (Table S1).

To determine the binding site(s) of the ligands, mutant TRPA1-expressing HEK293 cell lines were created. The residues mutated were chosen based on the functional groups on the ligands and the residues that could participate in either covalent modification (C621 [13]) or

through non-covalent aromatic interactions (F909 [16] and F944 [17]). C621A-hTRPA1 showed significantly reduced agonism responses for electrophilic compounds, in line with previous reports [11, 12]. We also observed significantly diminished agonism with non-reactive compounds. A similar type of effect had been previously described for menthol, NPPB and FTS [35]. However the reduced effects observed with NPPB and FTS in the mutant C621A were not statistically significant, though a significant reduction in agonism was observed with the mutations of different cysteine residues at the *N*-terminus [35, 61]. The TRPA1 antagonists could not be evaluated in this mutant, since the hTRPA1 standard agonists CA, AITC and ACR bind to the mutated site. In addition to the ^{1}H NMR study carried out with CAD **1a**, the findings with the C621A mutant further suggest that CADs do not undergo covalent modification at the TRPA1 *N*-terminal cysteine. The reduced agonism observed for CAD **22a** is however an anomaly, but this can be explained by chemical reactivity observed for this ester. When attempting to hydrolyse **22a**, to get the free acid, the compound eliminated the phenoxy group, presumably *via* an E1cb mechanism, to yield an acrylamide derivative. With reduced conjugation and no β-substituent, this compound would be expected to be much more likely to undergo covalent addition reaction compared to a cinnamide. Thus, the change in modulation of **22a** in the C621A mutant could be explained if such a process also takes place inside the cell.

For F909A-hTRPA1, significantly reduced inhibition was observed as expected for A967079 relative to the WT-hTRPA1 response [16]. Significantly reduced antagonism was also observed for the structurally similar oxime AP18. Since the tested antagonists with distinct structures, including CAD **13** and ASD, also showed significant differences in this mutant, F909 residue appears to be a key residue for antagonist binding in hTRPA1. Both CAD **13**, ASD and HC030031 incorporate two aromatic rings joined by a linking group. The

505 reduced antagonism was not observed for HC030031, but this could be explained by the fact
506 that the aromatic methyl xanthine half of the molecule is a larger bicyclic heteroaromatic ring
507 structure, as opposed to a single benzenoid rings in CAD **13** and ASD; it is therefore likely to
508 have a different binding site. There was also a drop in the agonism of menthol and carvacrol
509 in the absence of the F909. As menthol lacks aromaticity and cannot participate in aromatic π
510 interactions, it appears a more general hydrophobic interaction may be involved here,
511 possibly also involving residues neighbouring F909, such as T874. For most of the other
512 compounds the responses were significantly higher than that observed in WT-hTRPA1. This
513 could be due to changes in the structural conformation of hTRPA1 as a result of the
514 substitution of the aromatic residue F909 to alanine.
515
516 The mutant F944A-hTRPA1-HEK293 cells displayed a significantly reduced response to
517 many of the ligands evaluated, including the non-aromatic compounds ACR and menthol that
518 cannot participate in π-π interactions. The cryo-EM structure of TRPA1 shows that F944 is
519 buried within the channel structure [16], and apparently closed to binding without
520 reorganization of the channel structure. Samanta *et al* [62] used limited proteolysis and mass
521 spectrometry to evaluate the effect of a small number of non-electrophilic channel modulators
522 (menthol, antagonist A967079, and agonist PF-4840154) on mouse TRPA1. In that work,
523 several regions of TRPA1 were proposed as experiencing conformational change upon
524 binding of the ligands studied. However, F944 and the S5 and S6 helices were not amongst
525 those implicated. Nevertheless our results, using a wider range of modulators and with
526 hTRPA1, indicate that it is possible that the reduced activities observed for our F944A
527 mutant is also indicative of significant structural reorganizations of the S5 and S6 helices
528 upon ligand binding. The responses obtained for A967079 in both F909 and F944 mutants
529 were equal. However, the analogue AP18 had significant differences in response despite the

close similarity in their structures; the AP18 inhibition was nearly abolished in the mutant F944A, but not in F909A. ASD, however, preferentially binds F909 over F944, possibly due to its greater size, site accessibility and location of the amino acid in the channel structure.

The residues F909 and F944 from each TRPA1 subunit are located in a 'ring' amongst the S5 and S6 helices, a portion of the channel which is thought to be membrane bound [16] (Fig. 8a-c). F909 is located at the bottom of a shallow pocket, whereas F944 is buried within the tertiary structure of the channel (Fig. 8c-d). Whilst previously EM studies have suggested the location of the A967079 binding site [16], this area is buried behind the F909 residue in the atomic model 3J9P. The drop-in activities of modulators in F909A and F944A demonstrated that the corresponding compounds may possibly bind to the aromatic phenylalanine in the hTRPA1 putative pore region non-covalently *via* π-π stacking and/or hydrophobic interactions. Whilst further structural biology will be needed to elucidate detailed ligand binding, derivatives with hydroxy groups, anthranilic acid derivatives such as non-steroidal anti-inflammatory drugs, CADs and aryl sulfonamide derivatives, showed significant reductions in responses in the mutant F944A, suggesting this residue might serve as a general determinant in the modulation of hTRPA1. Complete elimination of the responses were not observed with most of the ligands suggesting they may also interact with other nearby residues.

The most potent CADs (**3**, **5** and **13**) were also characterized on isolated guinea pig vagus nerves. Unfortunately, the potency seen in the TRPA1-HEK293 cells was not observed in the nerve tissue. ACR was used as the TRPA1 standard agonist to determine the inhibitory effects of the compounds in guinea pig vagus nerve tissue, as desensitization of responses were observed with the use of CA in depolarization measurements [45, 63]. As a positive control, incubation with the TRPA1 standard antagonist HC030031 inhibited the

depolarization induced by ACR. However, contrary to the antagonistic effects observed in hTRPA1-HEK293 cells, neither of the compounds **5** and **13** exhibited any antagonism against depolarization of the guinea pig vagus nerve by ACR. This discrepancy in results could be due to, but not limited to, experimental differences or a consequence of species difference. There is only 79% identity between the amino acid sequences of hTRPA1 and guinea pig TRPA1. The low sequence homology with 21% variation could cause differences in responses. Caffeine, menthol and thioaminals (e.g. 4-methyl-*N*-[2,2,2-trichloro-1-(4-nitro-phenylsulfanyl)-ethyl]-benzamide), are potent antagonists in hTRPA1 but showed reduced potency, agonism or inactivity in rodent TRPA1 [64-66]. Similarly, rodent TRPA1 is activated by cold, whereas human and rhesus monkey TRPA1 are not [67]. The menthol and cold species difference were attributed to a single residue, V875 in primates and G878 in rodents [67].

A possible correlation is also noted between the various observed biological activities of CADs and TRP channels. This is plausible due to the known participation of TRP channels in a wide range of cellular functions [68]. Key to this suggestion is a study [69] which reports that TRPA1 is necessary for TGF-β signaling. Loss of the receptor significantly suppresses the mRNA expression of the inflammatory cytokines, IL-6, α-smooth muscle actin involved in fibrosis, substance P involved in inflammation, VEGF, collagen Iα1 and the phosphorylation of kinases induced by TGF-β, and thereby results in attenuation of fibrogenic and inflammatory reactions. Likewise, in the literature, the anti-allergic, anti-inflammatory [18, 19], anti-oxidant [20], anti-fibrotic [70], anti-proliferative [22] and anti-cancer [23] properties of CADs were related to inhibition of cytokines, chemokines and growth factors. Therefore the fundamental reason behind attenuation of cytokines and growth factors by CADs, might be the consequence of effects imposed by CADs on TRP channels.

5. Conclusions

The series of CADs possess various activities in hTRPA1, ranging from agonism, partial agonism, antagonism and desensitizing effects. The structurally related compound, ACA, an inhibitor of TRPM2, TRPM8, TRPC3, TRPC6 and TRPV1 [32] activates hTRPA1 with similar potency to those of other CADs evaluated in the study. CAD **13** (*p*-OH), with a strong EDG-substituent, and CAD **21** (α-Ph), show promise as a selective hTRPA1 antagonist and agonist, respectively. Using the key SARs found in the study, the structures of the compounds could be optimized to make CADs more potent modulators of TRPA1. Moreover, F944 was found to be a key residue for many TRPA1 active modulators, including menthol, anthranilates including fenamates and CADs, and ASD. Activity for these modulators was much reduced in the F944A mutant, indicating that this and other residues (F909) within the TRPA1 S5-S6 putative pore region are crucial for chemosensation.

Conflicts of Interest

The authors declare no conflict of interest.

Author Contributions

A.C., L.R.S., A.N.B. and A.H.M. designed the study overall. A.C. performed the chemical and pharmacology experiments, and wrote the initial draft of the manuscript. L.R.S., A.N.B., A.C. and A.H.M. contributed to the interpretation of the chemical and pharmacological data, and M.J.McP. performed the molecular modelling study and interpretation of the combined results therefrom. The final manuscript was reviewed and approved by all authors.

Acknowledgements

Thanks are due to Dr Kevin Morgan for his guidance with the pharmacology, Dr Kevin Welham, Mrs Carol Kennedy, Mr Daniel Mackenzie-Wade and Mr Christopher Crow for their technical support. We thank Prof Colin Fishwick (University Leeds) for useful discussions. We are also grateful to Dr Sara Bonvini, Dr Mark Birrell and Prof. Maria Belvisi of IR Pharma (http://www.irpharma.co.uk/), for designing and performing the guinea pig vagus nerve experiments. This research was supported by the University of Hull with a tuition fee bursary to AC.

Supporting Information

The following supplementary data to this article can be found online at: http://xxxxxxxxxxxx

1. Chemical synthesis procedures. 2. Characterization data: NMR, MS, EA and m.p. for the compounds synthesized. 3. Table S1: Physicochemical properties of the CADs evaluated. 4. ^{1}H and ^{13}C NMR spectra of the compounds prepared.

References

[1] D. Jaquemar, T. Schenker, B. Trueb, An ankyrin-like protein with transmembrane domains is specifically lost after oncogenic transformation of human fibroblasts, Journal of Biological Chemistry 274 (1999) 7325–7333.
[2] G.M. Story, A.M. Peier, A.J. Reeve, S.R. Eid, J. Mosbacher, T.R. Hricik, T.J. Earley, A.C. Hergarden, D.A. Andersson, S.W. Hwang, P. McIntyre, T. Jegla, S. Bevan, A. Patapoutian, ANKTM1, a TRP-like channel expressed in nociceptive neurons, is activated by cold temperatures, Cell 112 (2003) 819–829.
[3] M.M. Salas, K.M. Hargreaves, A.N. Akopian, TRPA1-mediated responses in trigeminal sensory neurons: interaction between TRPA1 and TRPV1, European Journal of Neuroscience 29 (2009) 1568–1578.
[4] J. Hjerling-Leffler, M. Alqatari, P. Ernfors, M. Koltzenburg, Emergence of functional sensory subtypes as defined by transient receptor potential channel expression, The Journal of Neuroscience 27 (2007) 2435–2443.
[5] M. Brozmanova, F. Ru, L. Surdenikova, L. Mazurova, T. Taylor-Clark, M. Kollarik, Preferential activation of the vagal nodose nociceptive subtype by TRPA1 agonists in the guinea pig esophagus, Neurogastroenterology and Motility 23 (2011) e437–445.
[6] P.M. Zygmunt, E.D. Högestätt, Mammalian transient receptor potential (TRP) cation channels, in: B. Nilius, V. Flockerzi (Eds.) Handbook of Experimental Pharmacology, Springer-Verlag, Berlin Heidelberg, 2014, pp. 583–630.
[7] D.M. Bautista, S.E. Jordt, T. Nikai, P.R. Tsuruda, A.J. Read, J. Poblete, E.N. Yamoah, A.I. Basbaum, D. Julius, TRPA1 mediates the inflammatory actions of environmental irritants and proalgesic agents, Cell 124 (2006) 1269–1282.
[8] B. Liu, J. Escalera, S. Balakrishna, L. Fan, A.I. Caceres, E. Robinson, A. Sui, M.C. McKay, M.A. McAlexander, C.A. Herrick, S.E. Jordt, TRPA1 controls inflammation and pruritogen responses in allergic contact dermatitis, FASEB Journal 27 (2013) 3549–3563.
[9] A. Horvath, V. Tekus, M. Boros, G. Pozsgai, B. Botz, E. Borbely, J. Szolcsanyi, E. Pinter, Z. Helyes, Transient receptor potential ankyrin 1 (TRPA1) receptor is involved in chronic arthritis: in vivo study using TRPA1-deficient mice, Arthritis Research & Therapy 18 (2016) 6.
[10] B.F. Bessac, S.E. Jordt, Breathtaking TRP channels: TRPA1 and TRPV1 in airway chemosensation and reflex control, Physiology 23 (2008) 360–370.
[11] A. Hinman, H.H. Chuang, D.M. Bautista, D. Julius, TRP channel activation by reversible covalent modification, Proceedings of the National Academy of Sciences of the United States of America 103 (2006) 19564–19568.
[12] L.J. Macpherson, A.E. Dubin, M.J. Evans, F. Marr, P.G. Schultz, B.F. Cravatt, A. Patapoutian, Noxious compounds activate TRPA1 ion channels through covalent modification of cysteines, Nature 445 (2007) 541–545.
[13] P.K. Bahia, T.A. Parks, K.R. Stanford, D.A. Mitchell, S. Varma, S.M. Stevens, T.E. Taylor-Clark, The exceptionally high reactivity of Cys 621 is critical for electrophilic activation of the sensory nerve ion channel TRPA1, Journal of General Physiology 147 (2016) 451–465.
[14] B. Xiao, A.E. Dubin, B. Bursulaya, V. Viswanath, T.J. Jegla, A. Patapoutian, Identification of transmembrane domain 5 as a critical molecular determinant of menthol sensitivity in mammalian TRPA1 channels, The Journal of Neuroscience 28 (2008) 9640–9651.
[15] K. Nakatsuka, R. Gupta, S. Saito, N. Banzawa, K. Takahashi, M. Tominaga, T. Ohta, Identification of molecular determinants for a potent mammalian TRPA1 antagonist by utilizing species differences, Journal of Molecular Neuroscience 51 (2013) 754–762.

[16] C.E. Paulsen, J.P. Armache, Y. Gao, Y. Cheng, D. Julius, Structure of the TRPA1 ion channel suggests regulatory mechanisms, Nature 520 (2015) 511–517.
[17] G. Klement, L. Eisele, D. Malinowsky, A. Nolting, M. Svensson, G. Terp, D. Weigelt, M. Dabrowski, Characterization of a ligand binding site in the human transient receptor potential ankyrin 1 pore, Biophysical Journal 104 (2013) 798–806.
[18] K. Harita, Y. Ajisawa, K. Iizuka, Y. Kinoshita, T. Kamijo, M. Kobayashi, Aromatic carboxylic amide derivatives, US3940422A (1976).
[19] M. Spiecker, I. Lorenz, N. Marx, H. Darius, Tranilast inhibits cytokine-induced nuclear factor κB activation in vascular endothelial cells, Molecular Pharmacology 62 (2002) 856–863.
[20] Y. Miyachi, S. Imamura, Y. Niwa, The effect of tranilast of the generation of reactive oxygen species, Journal of Pharmacobio-Dynamics 10 (1987) 255–259.
[21] D.J. Kelly, S.J. Williams, S. Zammit, Halogenated analogues of anti-fibrotic agents, WO2009079692A1 (2009).
[22] H. Ogita, Y. Isobe, H. Takaku, R. Sekine, Y. Goto, S. Misawa, H. Hayashi, Synthesis and structure-activity relationship of diarylamide derivatives as selective inhibitors of the proliferation of human endothelial cells, Bioorganic & Medicinal Chemistry 10 (2002) 3473–3480.
[23] D. Raffa, B. Maggio, F. Plescia, S. Cascioferro, S. Plescia, M.V. Raimondi, G. Daidone, M. Tolomeo, S. Grimaudo, A. Di Cristina, R.M. Pipitone, R. Bai, E. Hamel, Synthesis, antiproliferative activity, and mechanism of action of a series of 2-{[(2E)-3-phenylprop-2-enoyl]amino}benzamides, European Journal of Medicinal Chemistry 46 (2011) 2786–2796.
[24] Y. Iwasa, T. Iwasa, K. Matsui, T. Yoshimura, N. Tanaka, K. Miyazaki, Anti-platelet action of an anti-allergic agent, N-(3',4'-dimethoxycinnamoyl)anthranilic acid (tranilast), European Journal of Pharmacology 120 (1986) 231–234.
[25] K. Miyazawa, J. Fukuyama, K. Misawa, S. Hamano, A. Ujiie, Tranilast antagonizes angiotensin II and inhibits its biological effects in vascular smooth muscle cells, Atherosclerosis 121 (1996) 167–173.
[26] L. Steinman, M. Platten, P.-K. Ho, M.L. Selley, Tranilast as modulator of T cell functioning for use in the treatment of autoimmune diseases, EP2253313A1 (2010).
[27] M.L. Selley, J.J. Inglis, R.O. Williams, A method of modulating B cell functioning, WO2006053390 (2006).
[28] N.L. Occleston, S. O'Kane, N. Goldspink, M.W. Ferguson, New therapeutics for the prevention and reduction of scarring, Drug Discovery Today 13 (2008) 973–981.
[29] M. Bandell, G.M. Story, S.W. Hwang, V. Viswanath, S.R. Eid, M.J. Petrus, T.J. Earley, A. Patapoutian, Noxious cold ion channel TRPA1 is activated by pungent compounds and bradykinin, Neuron 41 (2004) 849–857.
[30] H. Hu, J. Tian, Y. Zhu, C. Wang, R. Xiao, J.M. Herz, J.D. Wood, M.X. Zhu, Activation of TRPA1 channels by fenamate nonsteroidal anti-inflammatory drugs, Pflügers Archiv: European Journal of Physiology 459 (2010) 579–592.
[31] L. Liu, Regulation of lung surfactant secretion by phospholipase A_2, Journal of Cellular Biochemistry 72 (1999) 103–110.
[32] C. Harteneck, H. Frenzel, R. Kraft, N-(p-Amylcinnamoyl)anthranilic acid (ACA): a phospholipase A_2 inhibitor and TRP channel blocker, Cardiovascular Drug Reviews 25 (2007) 61–75.
[33] M.J. Gunthorpe, H.K. Rami, J.C. Jerman, D. Smart, C.H. Gill, E.M. Soffin, S. Luis Hannan, S.C. Lappin, J. Egerton, G.D. Smith, A. Worby, L. Howett, D. Owen, S. Nasir, C.H. Davies, M. Thompson, P.A. Wyman, A.D. Randall, J.B. Davis, Identification and characterisation of SB-366791, a potent and selective vanilloid receptor (VR1/TRPV1) antagonist, Neuropharmacology 46 (2004) 133–149.

[34] A. Weil, S.E. Moore, N.J. Waite, A. Randall, M.J. Gunthorpe, Conservation of functional and pharmacological properties in the distantly related temperature sensors TRPV1 and TRPM8, Molecular Pharmacology 68 (2005) 518–527.
[35] K. Liu, M. Samuel, M. Ho, R.K. Harrison, J.W. Paslay, NPPB structure-specifically activates TRPA1 channels, Biochemical Pharmacology 80 (2010) 113–121.
[36] Orion Corp., New pharmaceutical compounds, EP20110165173 (2012).
[37] L.R. Sadofsky, B. Campi, M. Trevisani, S.J. Compton, A.H. Morice, Transient receptor potential vanilloid-1-mediated calcium responses are inhibited by the alkylamine antihistamines dexbrompheniramine and chlorpheniramine, Experimental Lung Research 34 (2008) 681–693.
[38] K. Morgan, L.R. Sadofsky, C. Crow, A.H. Morice, Human TRPM8 and TRPA1 pain channels, including a gene variant with increased sensitivity to agonists (TRPA1 R797T), exhibit differential regulation by SRC-tyrosine kinase inhibitor, Bioscience Reports 34 (2014) e00131.
[39] C. McClenaghan, F. Zeng, J.M. Verkuyl, TRPA1 agonist activity of probenecid desensitizes channel responses: consequences for screening, Assay and Drug Development Technologies 10 (2012) 533–541.
[40] J. Luo, Y. Zhu, M.X. Zhu, H. Hu, Cell-based calcium assay for medium to high throughput screening of TRP channel functions using FlexStation 3, Journal of Visualized Experiments : JoVE, 54 (2011) e3149.
[41] L.R. Sadofsky, A.N. Boa, S.A. Maher, M.A. Birrell, M.G. Belvisi, A.H. Morice, TRPA1 is activated by direct addition of cysteine residues to the N-hydroxysuccinyl esters of acrylic and cinnamic acids, Pharmacological Research 63 (2011) 30–36.
[42] C. Kilkenny, W.J. Browne, I.C. Cuthill, M. Emerson, D.G. Altman, Improving bioscience research reporting: the ARRIVE guidelines for reporting animal research, PLoS Biology 8 (2010) e1000412.
[43] M.A. Birrell, M.G. Belvisi, M. Grace, L. Sadofsky, S. Faruqi, D.J. Hele, S.A. Maher, V. Freund-Michel, A.H. Morice, TRPA1 agonists evoke coughing in guinea pig and human volunteers, American Journal of Respiratory and Critical Care Medicine 180 (2009) 1042–1047.
[44] S.A. Maher, M.A. Birrell, M.G. Belvisi, Prostaglandin E_2 mediates cough via the EP_3 receptor: implications for future disease therapy, American Journal of Respiratory and Critical Care Medicine 180 (2009) 923–928.
[45] Y.A. Alpizar, M. Gees, A. Sanchez, A. Apetrei, T. Voets, B. Nilius, K. Talavera, Bimodal effects of cinnamaldehyde and camphor on mouse TRPA1, Pflügers Archiv: European Journal of Physiology 465 (2013) 853–864.
[46] C.D. Lindsay, C. Green, M. Bird, J.T.A. Jones, J.R. Riches, K.K. McKee, M.S. Sandford, D.A. Wakefield, C.M. Timperley, Potency of irritation by benzylidenemalononitriles in humans correlates with TRPA1 ion channel activation, Royal Society Open Science 2 (2015) 140160–140177.
[47] J.B. Schachter, S.M. Sromek, R.A. Nicholas, T.K. Harden, HEK293 human embryonic kidney cells endogenously express the $P2Y_1$ and $P2Y_2$ receptors, Neuropharmacology 36 (1997) 1181–1187.
[48] S.P. Yu, G.A. Kerchner, Endogenous voltage-gated potassium channels in human embryonic kidney (HEK293) cells, Journal of Neuroscience Research 52 (1998) 612–617.
[49] B. Jiang, X. Sun, K. Cao, R. Wang, Endogenous Kv channels in human embryonic kidney (HEK-293) cells, Molecular and Cellular Biochemistry 238 (2002) 69–79.
[50] O. Moran, M. Nizzari, F. Conti, Endogenous expression of the β1A sodium channel subunit in HEK-293 cells, FEBS Letters 473 (2000) 132–134.

766 [51] B. He, D.M. Soderlund, Human embryonic kidney (HEK293) cells express endogenous
767 voltage-gated sodium currents and $Na_v1.7$ sodium channels, Neuroscience Letters 469 (2010)
768 268–272.
769 [52] D. Meyer zu Heringdorf, H. Lass, I. Kuchar, M. Lipinski, R. Alemany, U. Rumenapp,
770 K.H. Jakobs, Stimulation of intracellular sphingosine-1-phosphate production by G-protein-
771 coupled sphingosine-1-phosphate receptors, European Journal of Pharmacology 414 (2001)
772 145–154.
773 [53] S. Berjukow, F. Doring, M. Froschmayr, M. Grabner, H. Glossmann, S. Hering,
774 Endogenous calcium channels in human embryonic kidney (HEK293) cells, British Journal
775 of Pharmacology 118 (1996) 748–754.
776 [54] V. Bugaj, V. Alexeenko, A. Zubov, L. Glushankova, A. Nikolaev, Z. Wang, E.
777 Kaznacheyeva, I. Bezprozvanny, G.N. Mozhayeva, Functional properties of endogenous
778 receptor- and store-operated calcium influx channels in HEK293 cells, Journal of Biological
779 Chemistry 280 (2005) 16790–16797.
780 [55] T.K. Zagranichnaya, X. Wu, M.L. Villereal, Endogenous TRPC1, TRPC3, and TRPC7
781 proteins combine to form native store-operated channels in HEK-293 cells, Journal of
782 Biological Chemistry 280 (2005) 29559–29569.
783 [56] J. Luo, J.M. Busillo, J.L. Benovic, M_3 muscarinic acetylcholine receptor-mediated
784 signaling is regulated by distinct mechanisms, Molecular Pharmacology, 74 (2008) 338–347.
785 [57] D.D. McKemy, How cold is it? TRPM8 and TRPA1 in the molecular logic of cold
786 sensation, Molecular Pain 1 (2005) 16.
787 [58] Y. Karashima, N. Damann, J. Prenen, K. Talavera, A. Segal, T. Voets, B. Nilius,
788 Bimodal action of menthol on the transient receptor potential channel TRPA1, The Journal of
789 Neuroscience 27 (2007) 9874–9884.
790 [59] M. Takaishi, F. Fujita, K. Uchida, S. Yamamoto, M. Sawada Shimizu, C. Hatai Uotsu,
791 M. Shimizu, M. Tominaga, 1,8-Cineole, a TRPM8 agonist, is a novel natural antagonist of
792 human TRPA1, Molecular Pain 8 (2012) 86.
793 [60] S.P. Lee, M.T. Buber, Q. Yang, R. Cerne, R.Y. Cortes, D.G. Sprous, R.W. Bryant,
794 Thymol and related alkyl phenols activate the hTRPA1 channel, British Journal of
795 Pharmacology 153 (2008) 1739–1749.
796 [61] W.J. Redmond, L. Gu, M. Camo, P. McIntyre, M. Connor, Ligand determinants of fatty
797 acid activation of the pronociceptive ion channel TRPA1, PeerJ 2 (2014) e248.
798 [62] A. Samanta, J. Kiselar, R.A. Pumroy, S. Han, V.Y. Moiseenkova-Bell, Structural
799 insights into the molecular mechanism of mouse TRPA1 activation and inhibition, Journal of
800 General Physiology 150 (2018) 751–762.
801 [63] U. Anand, W.R. Otto, P. Facer, N. Zebda, I. Selmer, M.J. Gunthorpe, I.P. Chessell, M.
802 Sinisi, R. Birch, P. Anand, TRPA1 receptor localisation in the human peripheral nervous
803 system and functional studies in cultured human and rat sensory neurons, Neuroscience
804 Letters 438 (2008) 221–227.
805 [64] L. Klionsky, R. Tamir, B. Gao, W. Wang, D.C. Immke, N. Nishimura, N.R. Gavva,
806 Species-specific pharmacology of trichloro(sulfanyl)ethyl benzamides as transient receptor
807 potential ankyrin 1 (TRPA1) antagonists, Molecular Pain 3 (2007) 39.
808 [65] B.R. Bianchi, X.F. Zhang, R.M. Reilly, P.R. Kym, B.B. Yao, J. Chen, Species
809 comparison and pharmacological characterization of human, monkey, rat, and mouse TRPA1
810 channels, Journal of Pharmacology and Experimental Therapeutics 341 (2012) 360–368.
811 [66] J. Chen, P.R. Kym, TRPA1: the species difference, Journal of General Physiology 133
812 (2009) 623–625.
813 [67] J. Chen, D. Kang, J. Xu, M. Lake, J.O. Hogan, C. Sun, K. Walter, B. Yao, D. Kim,
814 Species differences and molecular determinant of TRPA1 cold sensitivity, Nature
815 Communications 4 (2013) 2501.

[68] D. Dadon, B. Minke, Cellular functions of transient receptor potential channels, The International Journal of Biochemistry & Cell Biology 42 (2010) 1430–1445.
[69] Y. Okada, K. Shirai, P.S. Reinach, A. Kitano-Izutani, M. Miyajima, K.C. Flanders, J.V. Jester, M. Tominaga, S. Saika, TRPA1 is required for TGF-β signaling and its loss blocks inflammatory fibrosis in mouse corneal stroma, Laboratory Investigation: a Journal of Technical Methods and Pathology 94 (2014) 1030–1041.
[70] K.D. James, W.S. John, Z. Steven, Halogenated analogues of anti-fibrotic agents, EP3045170A1 (2008).
[71] G. Chung, S.T. Im, Y.H. Kim, S.J. Jung, M.R. Rhyu, S.B. Oh, Activation of transient receptor potential ankyrin 1 by eugenol, Neuroscience 261 (2014) 153–160.
[72] W.J. Redmond, M. Camo, V. Mitchell, C.W. Vaughan, M. Connor, Nordihydroguaiaretic acid activates hTRPA1 and modulates behavioral responses to noxious cold in mice, Pharmacology Research & Perspectives 2 (2014) e00079.
[73] M. Maher, H. Ao, T. Banke, N. Nasser, N.T. Wu, J.G. Breitenbucher, S.R. Chaplan, A.D. Wickenden, Activation of TRPA1 by farnesyl thiosalicylic acid, Molecular Pharmacology 73 (2008) 1225–1234.
[74] W. Niforatos, X.F. Zhang, M.R. Lake, K.A. Walter, T. Neelands, T.F. Holzman, V.E. Scott, C.R. Faltynek, R.B. Moreland, J. Chen, Activation of TRPA1 channels by the fatty acid amide hydrolase inhibitor 3'-carbamoylbiphenyl-3-yl cyclohexylcarbamate (URB597), Molecular Pharmacology 71 (2007) 1209–1216.
[75] K. Talavera, M. Gees, Y. Karashima, V.M. Meseguer, J.A. Vanoirbeek, N. Damann, W. Everaerts, M. Benoit, A. Janssens, R. Vennekens, F. Viana, B. Nemery, B. Nilius, T. Voets, Nicotine activates the chemosensory cation channel TRPA1, Nature Neuroscience 12 (2009) 1293–1299.
[76] J. Chen, S.K. Joshi, S. DiDomenico, R.J. Perner, J.P. Mikusa, D.M. Gauvin, J.A. Segreti, P. Han, X.F. Zhang, W. Niforatos, B.R. Bianchi, S.J. Baker, C. Zhong, G.H. Simler, H.A. McDonald, R.G. Schmidt, S.P. McGaraughty, K.L. Chu, C.R. Faltynek, M.E. Kort, R.M. Reilly, P.R. Kym, Selective blockade of TRPA1 channel attenuates pathological pain without altering noxious cold sensation or body temperature regulation, Pain 152 (2011) 1165–1172.
[77] M. Petrus, A.M. Peier, M. Bandell, S.W. Hwang, T. Huynh, N. Olney, T. Jegla, A. Patapoutian, A role of TRPA1 in mechanical hyperalgesia is revealed by pharmacological inhibition, Molecular Pain 3 (2007) 40.
[78] C.R. McNamara, J. Mandel-Brehm, D.M. Bautista, J. Siemens, K.L. Deranian, M. Zhao, N.J. Hayward, J.A. Chong, D. Julius, M.M. Moran, C.M. Fanger, TRPA1 mediates formalin-induced pain, Proceedings of the National Academy of Sciences of the United States of America 104 (2007) 13525–13530.
[79] Orion Corporation, New pharmaceutical compounds, EP2520566A1 (2011).
[80] H. Wei, A. Koivisto, M. Saarnilehto, H. Chapman, K. Kuokkanen, B. Hao, J.-L. Huang, Y.-X. Wang, A. Pertovaara, Spinal transient receptor potential ankyrin 1 channel contributes to central pain hypersensitivity in various pathophysiological conditions in the rat, Pain 152 (2011) 582–591.

Figure and Scheme Legends

Scheme 1. Synthesis of *N*-cinnamoylanthranilate derivatives from cinnamic acids. The derivatives **1**-**8**, **13**-**17**, **20**, **21**, and their corresponding methyl *N*-cinnamoylanthranilate ester derivatives, including **22a**, were synthesized using this approach.

Scheme 2. Synthesis of *N*-cinnamoylanthranilic acid derivatives from aldehydes. The derivatives **9**-**12** were synthesized using this approach.

Scheme 3. Synthesis of *N*-cinnamoyl amino acids (rac-**18** and *S*-**19**).

Figure 1. Chemical structures of non-CAD TRPA1 modulators involved in this work.

Figure 2. Chemical structures of the *N*-cinnamoylanthranilate and related derivatives synthesized and evaluated in this study.

Figure 3. Dose-response curves of *N*-cinnamoylanthranilate derivatives in hTRPA1 (**a** - **f**) and hTRPM8 (**g**) HEK293 cells. Each data point on the curve represents the mean of three independent experiments ($N = 3$) in duplicates ($n = 6$) with their SEM.

Figure 4. Real-time spectrum recorded for 10 min (incubation period) for the compounds with bimodal activity (potent agonism and desensitization) in hTRPA1-HEK293 cells. **(a)** cinnamaldehyde (CA, 30 µM), **(b)** flufenamic acid (FFA, 100 µM), **(c)** *p*-Br CAD-**4** (10 µM), **(d)** *p*-Cl CAD-**5** (10 µM), **(e)** *o*-Cl CAD-**6** (10 µM) and **(f)** *p*-F CAD-**7** (10 µM). The concentration of CA in the second addition was 30 µM.

Figure 5. (a) Desensitizing effect and **(b)** reversibility of halogenated *N*-cinnamoylanthranilic acids **4**-**7** on hTRPA1-HEK293 cells. Each bar represents the mean ± SEM (N = 3, n = 6), and the statistical significance was determined using one-way ANOVA at $*p < 0.05$.

Figure 6. Screening results of TRPA1 ligands in the hTRPA1 mutants, F909A, F944A and C621A, and comparison of the responses against WT-hTRPA1 HEK293 cells, **(a-e)** agonism and **(f)** antagonism. Each bar represents the mean ± SEM of N = 3 (n = 6), and statistical significance was compared relative to WT at $*p < 0.05$, $**p < 0.01$, $***p < 0.001$ and $****p < 0.0001$, using one-way ANOVA; black stars indicate significant reduction and grey stars indicate significant increase in response relative to WT.

Figure 7. Effects of CADs **3**, **5** and **13** on isolated guinea pig vagus nerve preparations, **(a - c)** agonism and **(d)** antagonism against acrolein (ACR, 300 µM) induced depolarization; each bar represents the mean ± SEM (N = 4). **(e)** Antagonism of CADs **5** and **13** against acrolein (300 µM in human TRPA1-HEK293 cells; each bar represents the mean ± SEM (N = 3, n = 9).

Figure 8. A. Human TRPA1 atomic model 3J9P showing the location of residues F909 (red) and F944 (blue) as coloured spheres. These are located in the membrane portion of the channel. **B.** Top down view of the channel showing the central pore and the 'ring' of F909 and F944 residues. **C.** Close up of TRPA1 showing the F944 and F909 repeating residues. **D.** Close up with surface highlighting residues in red F909 (top) and T874 (bottom), and the location of the shallow pocket for putative antagonist binding. The location of F944 (blue) is buried and unavailable for ligand binding without significant structural movement.

Scheme 1.

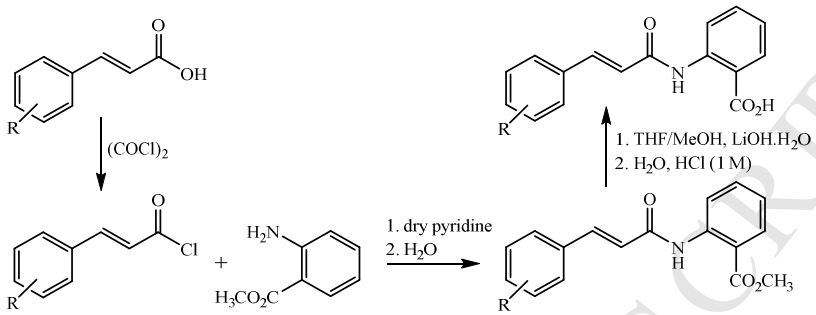

Scheme 2.

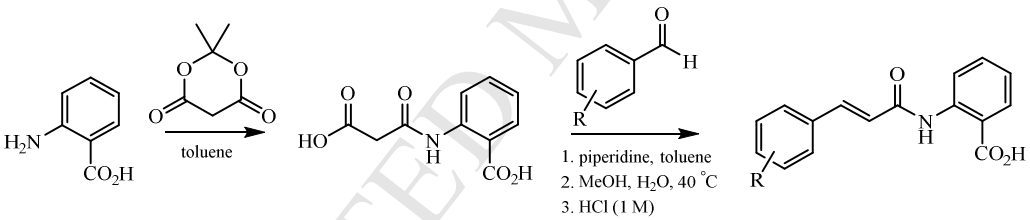

Scheme 3.

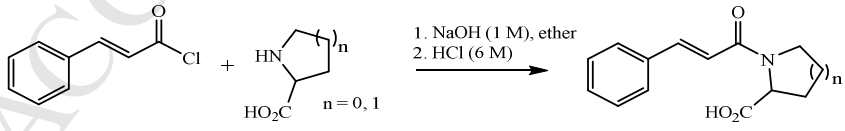

Table 1. Screening results of the synthesized *N*-cinnamoylanthranilic acids in hTRPA1 and hTRPM8-transfected HEK293 cells. The concentrations at which the compounds were tested are specified in the corresponding column title. Dose-response curves in hTRPA1 were carried out for the compounds that showed >25 % agonist activity at 30 µM, and that had partial agonism and high antagonism, in the initial screening. Dose-response curves in hTRPM8 were carried out for the compounds which showed >60 % inhibitory effect in the initial screening. For compounds where an EC_{50} or IC_{50} could not be calculated, a dash (-) is given instead of a value. Each value represents the mean ± SEM (*N* = 3).

Compound	**CAD variant**	**hTRPA1-HEK293**						**hTRPM8-HEK293**			
		Agonism / (% calcimycin) 30 µM *N* = 3 ± SEM	**Antagonism, CA response / (% CA) 100 µM *N* = 3 ± SEM**	**LogEC_{50} / (M) *n* = 6, *N* = 3 ± SEM**	**EC_{50} /(µM)**	**LogIC_{50} / (M) *n* = 6, *N* = 3 ± SEM**	**IC_{50} /(µM)**	**Agonism / (% calcimycin) 30 and 100 µM *N* = 3 ± SEM**	**Antagonism, WS5 response / (% WS5) 100 µM *N* = 3 ± SEM**	**LogIC_{50} / (M) *n* = 6, *N* = 3 ± SEM**	**IC_{50} /(µM)**
1	-	24 ± 1	42 ± 3	-	-	-	-	No agonism response was obtained for any of these compounds.	48 ± 6	-	-
2	4-NO_2	25 ± 1	33 ± 6	-3.7 ± 0.2	219	-	-		39 ± 7	-	-
3	4-CF_3	51 ± 1	28 ± 2	-4.57 ± 0.06	27	-	-		17 ± 3	-4.5 ± 0.2	34
4	4-Br	60 ± 3	6 ± 2	-4.94 ± 0.09	12	-5.0 ± 0.2	9		35 ± 2	-4.2 ± 0.4	59
5	4-Cl	62 ± 1	7 ± 1	-5.00 ± 0.07	10	-5.4 ± 0.1	4		40 ± 5	-	-
6	2-Cl	44 ± 2	5 ± 2	-4.37 ± 0.07	42	-5.0 ± 0.1	11		25 ± 4	-4.7 ± 0.5	21
7	4-F	37 ± 1	13 ± 4	-4.5 ± 0.1	30	-4.6 ± 0.1	26		61 ± 8	-	-
8	4-CH_3	30 ± 1	40 ± 1	-3.8 ± 0.1	149	-	-		48 ± 3	-	-
9	2-OCH_3	33 ± 1	14 ± 2	-4.1 ± 0.1	75	-4.3 ± 0.2	51		32 ± 8	-4.4 ± 0.3	41
10	4-OCH_3	27 ± 1	19 ± 6	-4.3 ± 0.2	49	-4.9 ± 0.1	12		68 ± 8	-	-
11	3,4-$(OCH_3)_2$	6 ± 3	56 ± 13	-	-	-3.9 ± 0.2	126		65 ± 6	-	-
12	3-OEt-4-OH	5 ± 1	34 ± 6	-	-	-4.0 ± 0.3	106		73 ± 6	-	-
13	4-OH	1 ± 1	35 ± 11	-	-	-4.4 ± 0.1	43		70 ± 5	-	-
14	3,4-$(OH)_2$	Fluorescing compounds							Fluorescing compounds		
15	4-$N(CH_3)_2$										
16	α,β-saturated	10 ± 3	81 ± 11	-	-	-	-		48 ± 4	-	-
17	α,β-saturated, 4-OCH_3	6 ± 1	74 ± 14	-	-	-	-		57 ± 5	-	-
18	Pipecolinic acid	7 ± 1	71 ± 9	-	-	-	-		72 ± 6	-	-
19	Proline	5 ± 2	79 ± 4	-	-	-	-		65 ± 5	-	-
20	α-CH_3	33 ± 2	29 ± 2	-3.9 ± 0.1	133	-	-		28 ± 7	-4.6 ± 0.2	27
21	α-Ph	66 ± 2	22 ± 1	-4.95 ± 0.04	11	-	-	14 ± 1, 34 ± 3	not measured	-	-

Table 2. Screening results of the methyl *N*-cinnamoylanthranilates (3 µM) in hTRPA1 and hTRPM8-HEK293 cells. As **2a** (4-NO_2) was insoluble in DMSO at room temperature, it was not evaluated. Each value represents the mean ± SEM (*N* = 3).

Compound	**CAD variant**	**hTRPA1-HEK293**		**hTRPM8-HEK293**	
		Agonism / / (% calcimycin) 3 µM *N* = 3 ± SEM	**Antagonism, CA response / (% CA) 3 µM *N* = 3 ± SEM**	**Agonism / (% calcimycin) 3 µM *N* = 3 ± SEM**	**Antagonism, WS5 response / (% WS5) 3 µM *N* = 3 ± SEM**
1a	-	22 ± 1	No inhibitory effect.	No agonism.	61 ± 1
3a	4-CF_3	29 ± 2			81 ± 11
4a	4-Br	41 ± 2			79 ± 4
5a	4-Cl	45 ± 2			70 ± 4
6a	2-Cl	29 ± 2			53 ± 1
7a	4-F	34 ± 3			85 ± 9
8a	4-CH_3	28 ± 3			88 ± 3
13a	4-OAc	10 ± 1			84 ± 2
14a	3,4-$(OAc)_2$	12 ± 1			102 ± 2
15a	4-$N(CH_3)_2$	27 ± 1			86 ± 22
20a	α-CH_3	49 ± 2	73 ± 7		30 ± 4
21a	α-Ph	63 ± 2	51 ± 2	23 ± 4	48 ± 7
22a	Phenoxy	45 ± 2 (at 30 µM)	No inhibitory effect.	No agonism	12 ± 2 (at 30 µM)

Table 3. The EC_{50} and IC_{50} values of the known ligands obtained in hTRPA1-HEK293 cells using a FlexStation, compared with the literature values of the original findings. Abbreviations: FLIPR, fluorometric imaging plate reader assay; EP, electrophysiology; FS, FlexStation; ND, not determined; NE, not estimable.

	Obtained value		**Literature value**
Ligand	**LogEC_{50} (M) ± SEM**	**EC_{50}**	**EC_{50}, species, assay [ref.]**
CA	-5.07 ± 0.09	9 µM	61 ± 9 µM, mouse TRPA1-CHO cells, FLIPR.[29]
ACR	-4.57 ± 0.07	27 µM	5 ± 1 µM, human TRPA1-*Xenopus oocytes*, EP.[7]
AITC	-5.36 ± 0.04	4 µM	22 ± 3 µM, mouse TRPA1-CHO cells, FLIPR.[29]
Menthol	-4.5 ± 0.1	30 µM	95 ± 15 µM, mouse TRPA1-CHO cells, EP.[58]
Thymol	-4.22 ± 0.06	60 µM	20 µM, human TRPA1-HEK293 cells, FLIPR.[60]
Carvacrol	-4.78 ± 0.09	17 µM	ND
Eugenol	-3.77 ± 0.09	168 µM	261 ± 9 µM, human TRPA1-HEK293 cells, EP.[71]
FFA	-5.16 ± 0.06	7 µM	24 ± 3 µM, WI-38 cells (human fibroblast), FS.[30]
			57 ± 5 µM, human TRPA1-HEK293 cells, FS.[30]
MFA	-4.78 ± 0.09	16 µM	61 ± 5 µM, WI-38 cells (human fibroblast), FS.[30]
DCF	-4.2 ± 0.1	56 µM	210 ± 22 µM, WI-38 cells (human fibroblast), FS.[30]
NPPB	-6.22 ± 0.09	0.6 µM	0.32 µM, human TRPA1-HEK293 cells, FLIPR.[35]
ACA	-4.55 ± 0.06	28 µM	ND
SB366791	inactive	-	ND
NDGA	-4.45 ± 0.08	35 µM	4.9 ± 1.7 µM, human TRPA1-HEK293 cells, FS.[72]
FTS	-6.08 ± 0.07	0.8 µM	7 ± 4 µM, human TRPA1-HEK293 cells, FLIPR.[73]
URB597	-0.87	0.1 µM	24.5 ± 3.2 µM, human TRPA1-HEK293F cells, FLIPR.[74]
Nicotine	0.34	2 M	~10 µM, mouse TRPA1-CHO cells, EP.[75]
Probenecid	NE	-	4.2 mM, human TRPA1-CHO cells, FS.[39]
Ligand	**LogIC_{50} ± SEM**	**IC_{50}**	**IC_{50}, species, assay**
A967079	-7.10 ± 0.09	79 nM	67 nM against AITC (30 µM), human TRPA1- HEK293F cells, FLIPR[76]
AP18	-5.35 ± 0.08	4 µM	3.1 µM against CA (50 µM), human TRPA1-CHO cells, FLIPR.[77]
HC030031	-4.75 ± 0.09	18 µM	6.2 ± 0.2 µM against AITC (5 µM), human TRPA1-HEK293 cells, fluorescence-based plate reader.[78]
ASD	-5.0 ± 0.1	10 µM	12.5 µM against AITC (5 µM), human TRPA1-HEK293 cells, FS.[79, 80]

Figure 1.

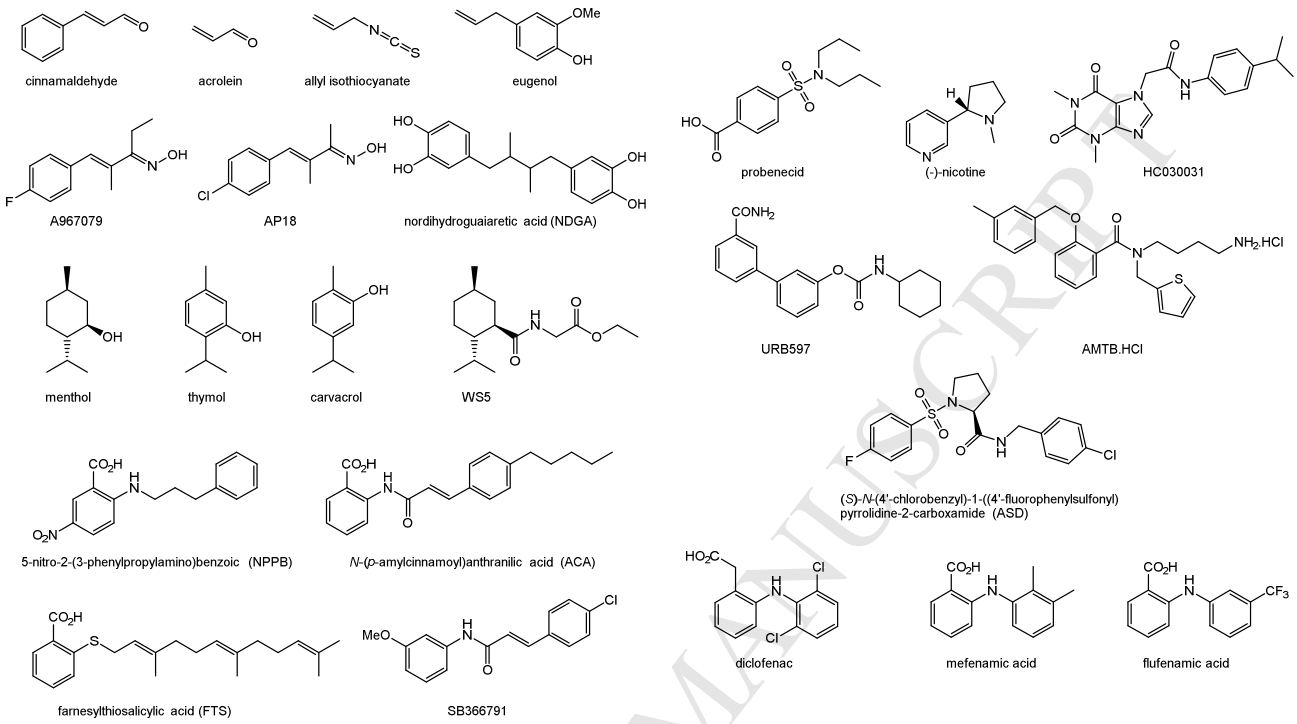

Figure 2

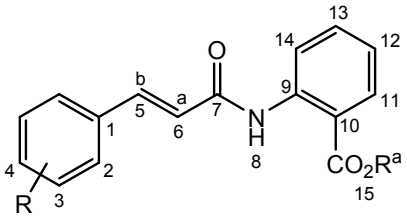

	R	R^a
1	H	H
2	4-NO_2	H
3	4-CF_3	H
4	4-Br	H
5	4-Cl	H
6	2-Cl	H
7	4-F	H
8	4-CH_3	H
9	2-OCH_3	H
10	4-OCH_3	H
11	3,4-$(OCH_3)_2$	H
12	3-OCH_2CH_3-4-OH	H
13	4-OH	H
14	3,4-$(OH)_2$	H
15	4-$N(CH_3)_2$	H

	R	R^a
1a	H	CH_3
2a	4-NO_2	CH_3
3a	4-CF_3	CH_3
4a	4-Br	CH_3
5a	4-Cl	CH_3
6a	2-Cl	CH_3
7a	4-F	CH_3
8a	4-CH_3	CH_3
13a	4-OAc	CH_3
14a	3,4-$(OAc)_2$	CH_3
15a	4-$N(CH_3)_2$	CH_3

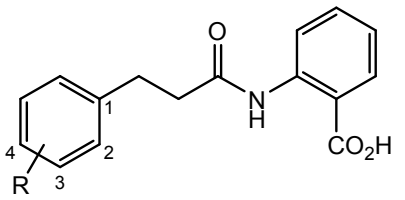

	R
16	H
17	4-OCH_3

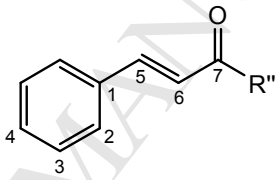

18

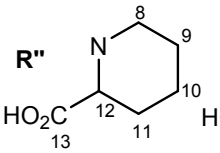

19

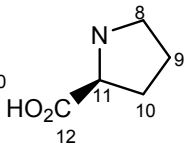

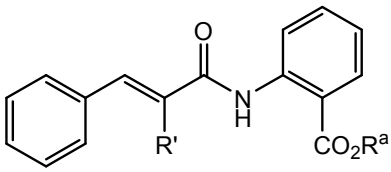

	R'	R^a
20	CH_3	H
21	Ph	H
20a	CH_3	CH_3
21a	Ph	CH_3

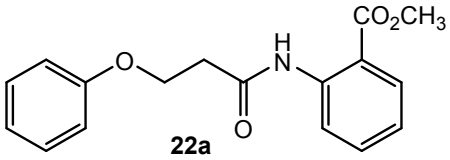

22a

Figure 3

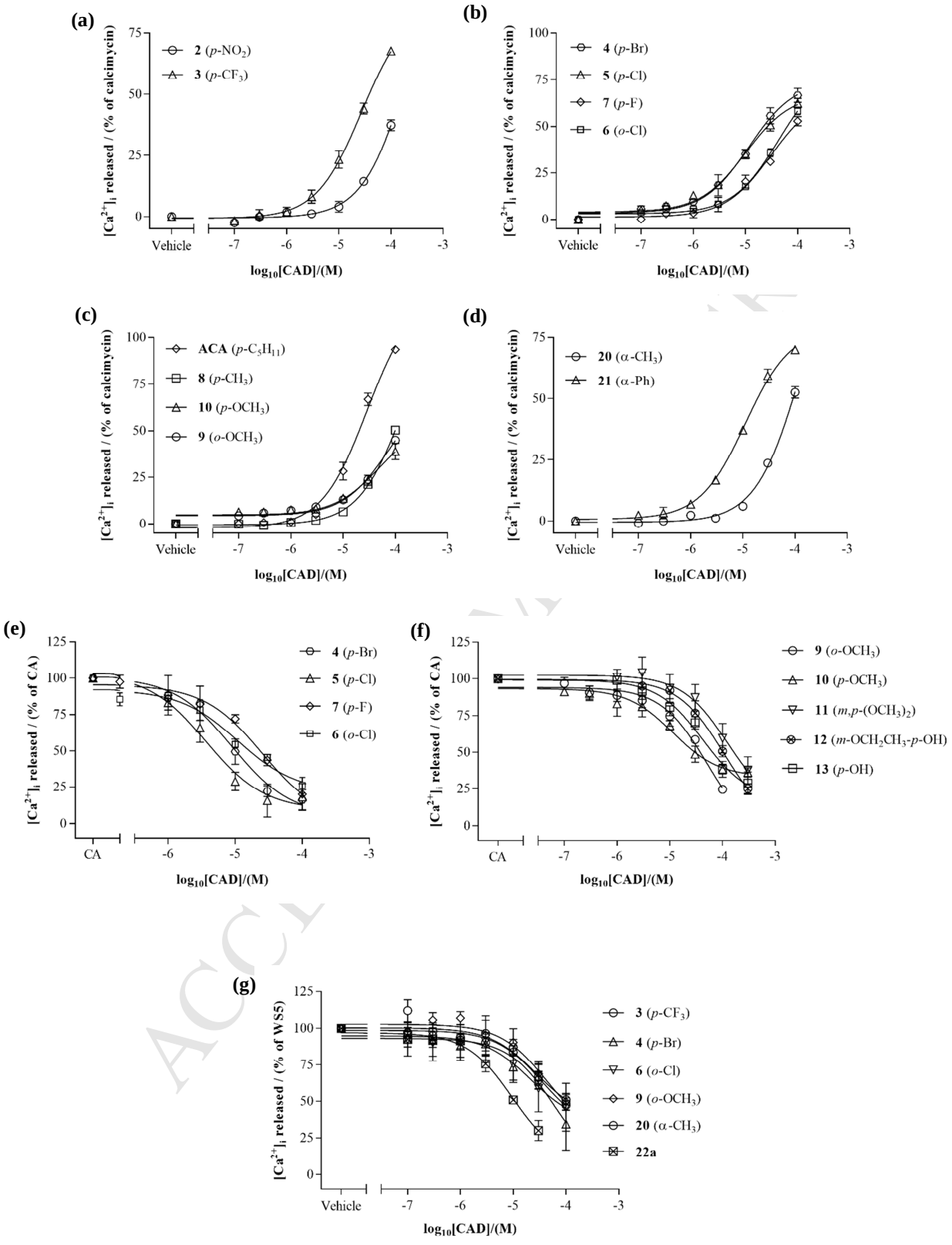
(a)
2 (p-NO2)
3 (p-CF3)
[Ca2+]i released / (% of calcimycin)
Vehicle
log10[CAD]/(M)
(b)
4 (p-Br)
5 (p-Cl)
7 (p-F)
6 (o-Cl)
(c)
ACA (p-C5H11)
8 (p-CH3)
10 (p-OCH3)
9 (o-OCH3)
(d)
20 (α-CH3)
21 (α-Ph)
(e)
[Ca2+]i released / (% of CA)
CA
(f)
9 (o-OCH3)
10 (p-OCH3)
11 (m,p-(OCH3)2)
12 (m-OCH2CH3-p-OH)
13 (p-OH)
(g)
[Ca2+]i released / (% of WS5)
3 (p-CF3)
4 (p-Br)
6 (o-Cl)
9 (o-OCH3)
20 (α-CH3)
22a

Figure 4

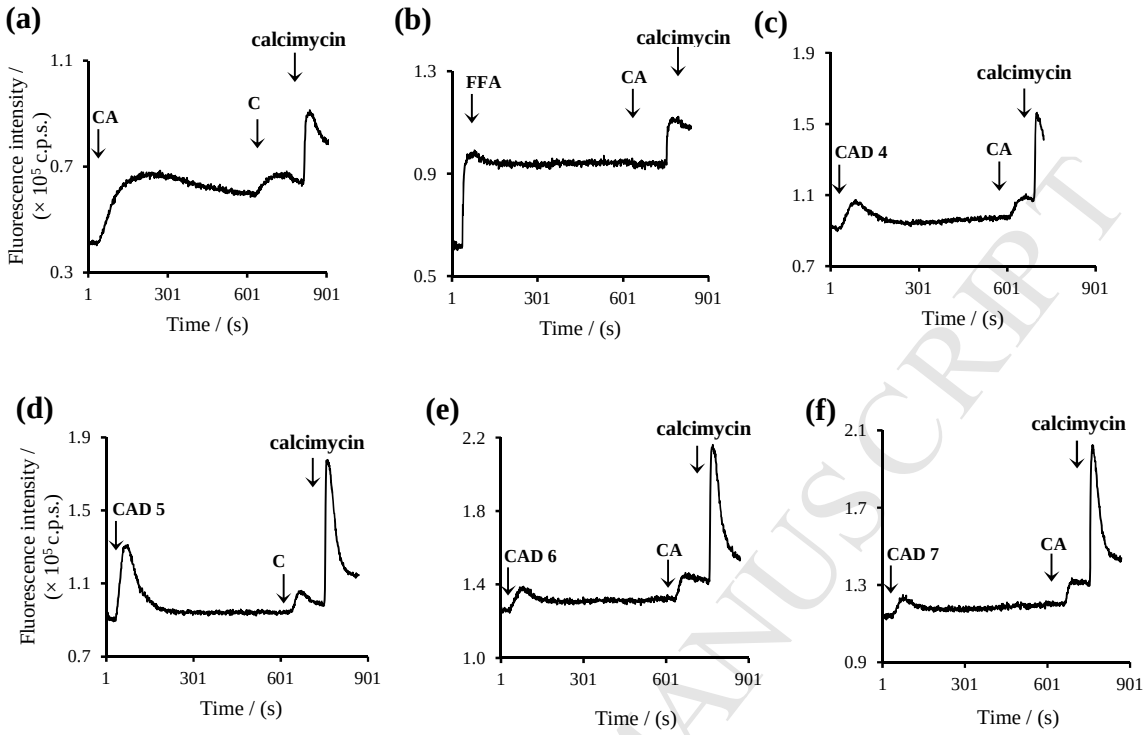

Figure 5

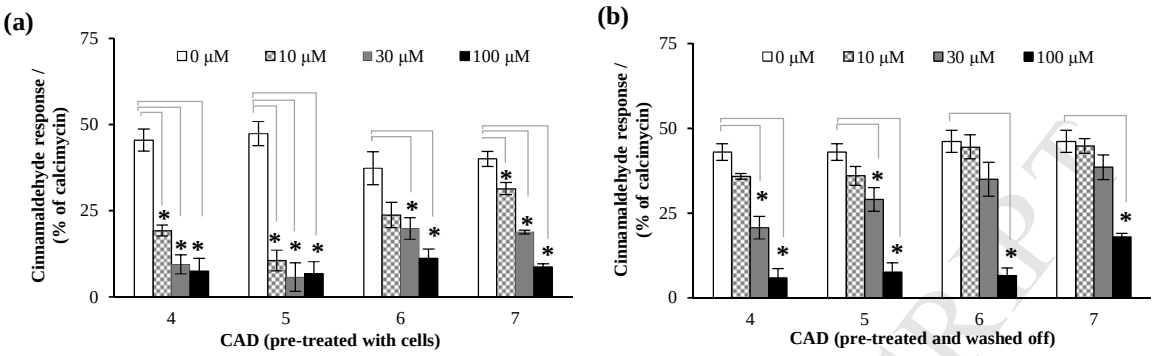

Figure 6

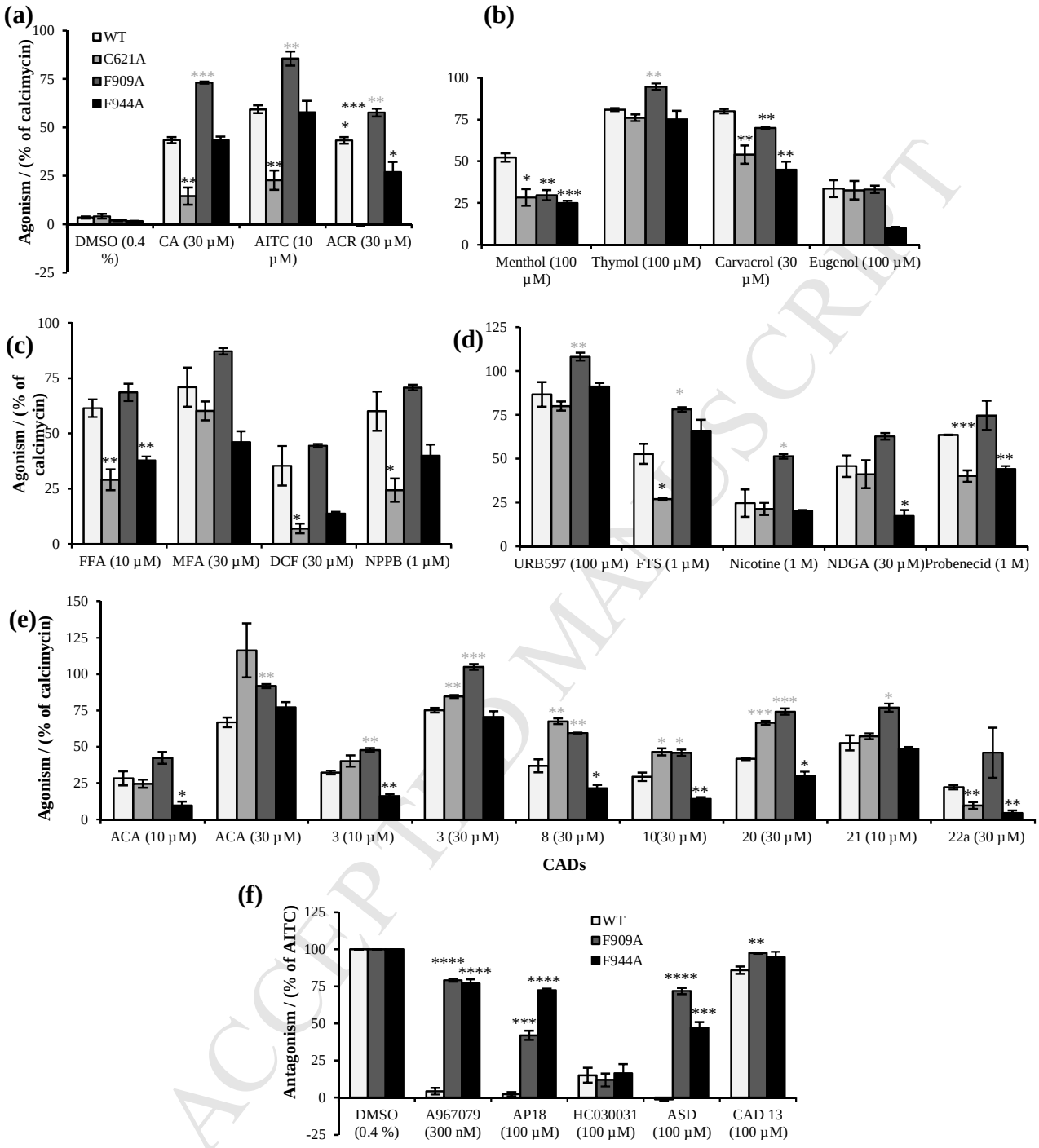

Figure 7

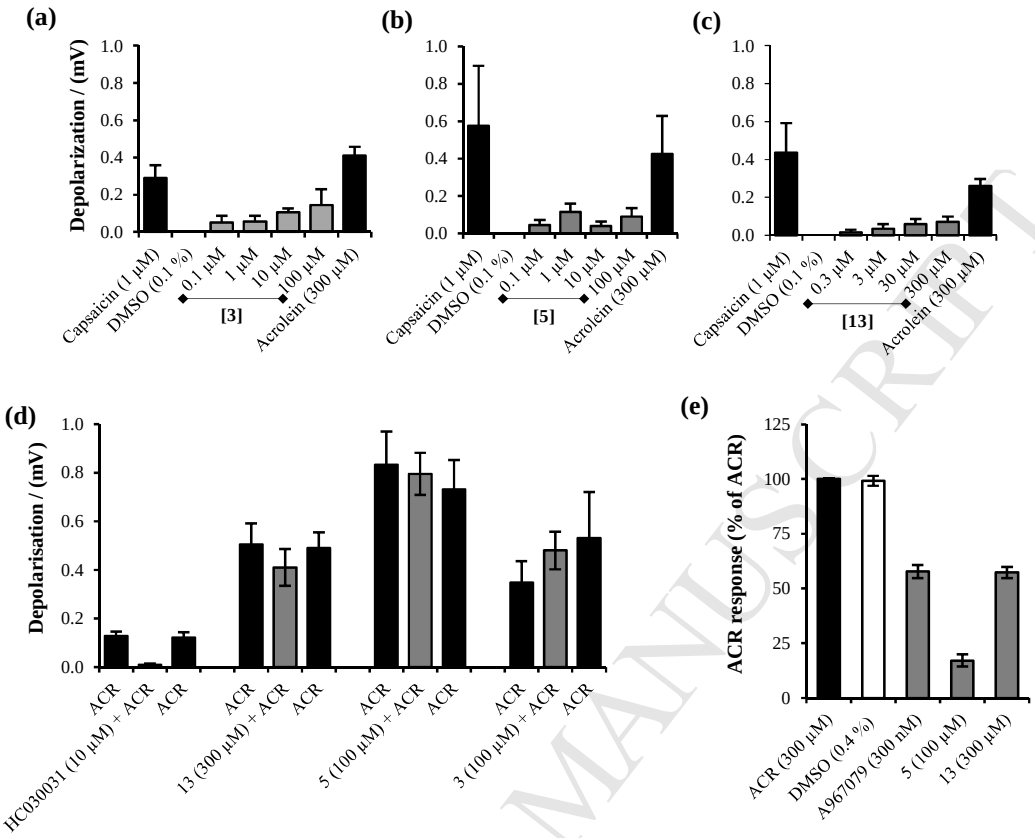

Figure 8